Restricted Phonon Relaxation and Anomalous Thermalization of Rare Earth Ions in Nanocrystals

ARTICLE *in* NANO LETTERS · MARCH 2002

Impact Factor: 13.59 · DOI: 10.1021/nl0255303

3 AUTHORS, INCLUDING:

G. K. Liu
Argonne National Laboratory
162 PUBLICATIONS **2,595** CITATIONS

NANO LETTERS

2002
Vol. 2, No. 5
535−539

Restricted Phonon Relaxation and Anomalous Thermalization of Rare Earth Ions in Nanocrystals

G. K. Liu,* H. Z. Zhuang, and X. Y. Chen

Chemistry Division, Argonne National Laboratory, Argonne, Illinois 60439

Received February 20, 2002; Revised Manuscript Received March 12, 2002

ABSTRACT

An anomalous thermalization effect induced by optical excitation of Er^{3+} ions in nanocrystals of Y_2O_2S is investigated. Due to the absence of low-energy phonon modes in the 20–40 nm crystals we studied, phonon relaxation is restricted, and as a result, the intensity of hot bands that originate from the upper crystal field levels in the $^4I_{15/2}$ ground state increases rapidly as temperature decreases below 8 K. This unusual increase in hot band intensity is interpreted satisfactorily by calculations of temperature dependent multiphonon relaxation rates in nanoparticles. Our theoretical analysis provides a fundamental understanding of confinement effects on the spectroscopic properties of rare earth ions in nanocrystals. This analysis applies also to the previously observed unusual hot bands in 4–6 nm particles of Eu_2O_3.

Although no quantum confinement should occur because of the localized electronic states, the optical spectrum and luminescence dynamics of an impurity ion in dielectric nanoparticles can be significantly modified through electron−phonon interaction. Confinement effects on electron−phonon interaction are primarily due to that the phonon density of states (PDOS) in a nanocrystal is discrete and the low-energy acoustic phonon modes are cut off. As a consequence of the PDOS confinement, luminescence dynamics of optical centers in nanoparticles, particularly, the nonradiative relaxation of ions from the electronically excited states, are expected to behave differently from that in bulk materials. Therefore, controlling of optical excitation and luminescence dynamics such as vibronic transitions and phonon-assisted energy transfer may be achieved through modification of the PDOS in nanostructured materials. In this regard, inorganic nanocrystals activated with rare earth or transition metal ions are of particular attraction because of their localized electronic states in which phonon influence is very sensitive. There have been extensive spectroscopic studies on the luminescence dynamics of rare earth ions in nanocrystals.[1−5] Recently, Tissue reported the observation of anomalous hot bands in the excitation spectra ($^7F_1$ to $^5D_1$) of Eu^{3+} ions in Eu_2O_3 nanocrystals, but no consistent explanation was provided.[1]

In this letter, we report an anomalous optical thermalization effect observed in laser excitation of Er^{3+} ions in nanocrystals of Y_2O_2S with diameters mostly between 20 and 40 nm. As temperature decreases below 7 K, Er^{3+} population in the upper crystal field levels above the ground level increases rapidly until saturation is reached. No such effect was observed in the 400 nm crystals. An interpretation is provided based on calculations of size dependent PDOS and multiphonon relaxation rates of isolated Er^{3+} ions in the nanocrystals.

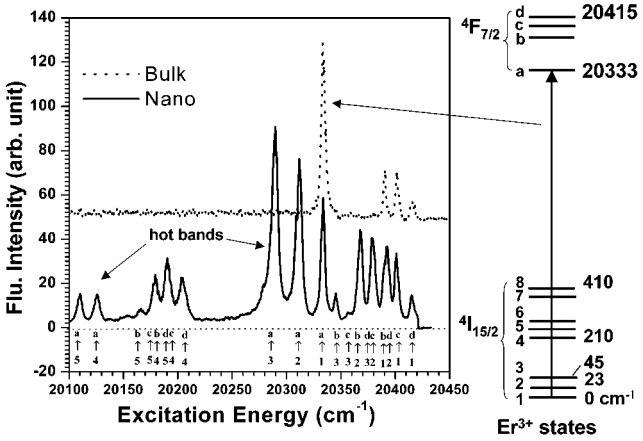

Figure 1. Excitation spectra of Er^{3+} in 10−40 nm diameters (solid curve) and 400 nm diameters (dashed curve) nanocrystals of Y_2O_2S at 2.6 K. The optical transition is from the $^4I_{15/2}$ ground state to the $^4F_{7/2}$ excited state above 20 300 cm^{-1}, whereas emission from the $^4S_{3/2}$ excited state at 18 248 cm^{-1} is monitored. The vertical arrows indicate the electronic transitions from the crystal field levels of ground state to that of the excited state. The fluorescence emission was detected using a boxcar integrator that averaged the fluorescence signal from a cooled PMT with 3 μs gate width and 1 μs delay from the laser pulse. The spectrometer bandwidth was set approximately at 0.5 cm^{-1}.

Figure 1 shows the low-temperature excitation spectra of Er^{3+} in bulk (400-nm) crystals and nanocrystals of Y_2O_2S, which were obtained by using a 5-ns pulse laser and

10.1021/nl0255303 CCC: $22.00
Published on Web 03/30/2002

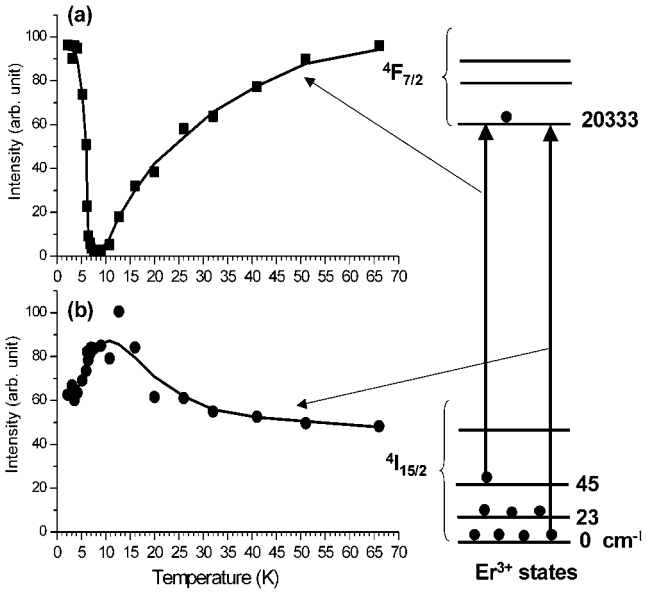

Figure 2. Temperature dependence of the excitation intensity of Er^{3+} in nanocrystals of Y_2O_2S: (a) the hot band originated from the crystal field level 45 cm^{-1} above the ground level, and (b) the normal excitation from the ground level.

monitoring the Er^{3+} fluorescence from the $^4S_{3/2}$ state at 18 248 cm^{-1}. At 2.6 K, the nanocrystal spectrum shows numerous hot bands originated from the upper Stark levels in addition to the four transitions from the lowest level of the $^4I_{15/2}$ ground state to the four levels of the $^4F_{7/2}$ excited state above 20 300 cm^{-1}, whereas the spectrum of the bulk-crystals consists of only four lines for the transitions from the bottom of the $^4I_{15/2}$ ground state.

The nanocrystals of Er^{3+}:Y_2O_2S were synthesized using a flame spray pyrolysis (FSP) method[6] and fluidized bed sulfidation process (FBS).[7] The samples we studied were characterized previously as of good crystalline lattice.[5] In our experiments, the crystalline powders of the two samples were sealed off in quartz cells filled with 1 Torr of helium gas. The two samples were mounted on the same sample holder in a cryostat for comparative studies. For measurements at temperatures below 4 K, the samples were actually in liquid helium, whereas the vapor gas was pumped to control the liquid temperature. The spectra shown in Figure 1 were obtained with peak intensity of the laser pulse at 500 W/mm^2. The hot bands were observable at very weak laser peak intensity (<1 W/mm^2) as long as the normal excitation from the lowest level was observable.

More curiously, the intensity of saturated hot bands in the nanocrystals decreases rapidly to zero as temperature increases from 6 to 8 K, and then increases along with temperature in the same behavior as that of Boltzmann thermalization. Above 12 K, the nanocrystals and the bulk-crystals exhibit same thermodynamics. This unusual behavior is shown in Figure 2(a) with the integrated intensity of the hot band from the third crystal field level 45 cm^{-1} above the ground level. In comparison, Figure 2(b) shows the ground level excitation which has an opposite temperature dependence. The integrated intensity of the ground level excitation reaches a maximum at 8K when the hot bands diminish to their minimum, which suggests that the appearance of the hot bands is indeed due to the Er^{3+} population in the upper crystal field levels.

To interpret the observed phenomena, we need address two questions: (1) how the initially empty upper levels are populated at temperatures of thermal energy far below the energy gaps of the electronic states (up to 200 cm^{-1}); and (2) why this anomalous thermalization occurs below 8 K in the nanocrystals but is absent in the bulk crystals.

Except for the novel behavior of the hot bands in the nanocrystals, the characteristics of the Er^{3+} crystal field spectrum are well understood.[8,9] In crystals, the localized 4f electrons of rare earth ions are weakly coupled to the lattice field, so that electronic transitions between the crystal field states within the 4f configuration have very sharp spectra. At liquid helium temperatures, a typical line width of the 4f−4f transitions is only on the order of 1 cm^{-1}. Due to inhomogeneous line broadening in glasses and structure-disordered solids, the inhomogeneous line width of 4f spectra increases to 100 cm^{-1} or broader. In nanocrystals, the influence of lattice defects and contamination of hydrous species in the considerably large area of surface layer is not negligible. It induces inhomogeneous broadening like that in glasses. In the particle center ions should have unperturbed crystalline lattice environment. Without selective excitation and fluorescence line narrowing, the 4f spectra from nanocrystals include contributions from ions in the surface layer as well as from the ions in the particle center. In Figure 1, the broad feature in the spectrum of the nanocrystals is indicated as the area above the dashed horizontal line, and it is attributed to the Er^{3+} ions at defect sites in the surface layer, whereas the sharp lines are due to the ions in the center.

The broad-band excitation, which is a consequence of particle size reduction, is essential for understanding the complicated luminescence dynamics and anomalous thermalization effect. The spectrum indicates that the hot bands originated from the upper crystal field levels are overlapped "accidentally" with the excitation of some defect sites from the lowest level in the ground state. In our experiments, when the laser was tuned to induce a resonant transition apparently from an upper level of the ground state which was initially empty at liquid helium temperatures, it actually pumped the Er^{3+} ions at defect sites from the ground level with excitation energy accidentally at the same level as that of the Er^{3+} ions at the intrinsic site from the upper crystal field levels. Through energy transfer and cascade emission of phonons, which occur efficiently in less than 5 ns after the laser pulse, the relaxation of an excited Er^{3+} ion at a defect site may result in populating more than one Er^{3+} ions in the upper levels of the ground state. This is how an empty level is populated at low temperature. Then, the Er^{3+} ions in these upper levels can be excited by the same laser pulse, and depending on the rate of nonradiative phonon relaxation of ions in the upper levels, observation of hot bands is possible. This effect is similar to a photon avalanche[10,11] except that a threshold is not observed in the present work.

In normal conditions, direct phonon relaxation in solids is very efficient and thermal population of ions in upper

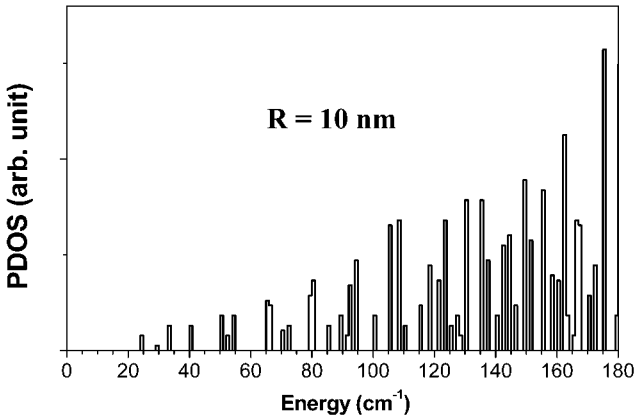

Figure 3. Calculated phonon density of states in 20-nm nanocrystal of Y_2O_2S.

electronic states obeys Boltzmann distribution: $n = n_0\exp(-E/kT)$. Therefore, no hot bands are observed from the states with energy level E much higher than kT. This is what we observed in the sample of 400-nm crystals. However, the Debye approximation of continuous distribution of PDOS is no longer valid for nanocrystals, in which vibrational modes become discrete, and no phonon modes exist below a cutoff energy in the low-energy side of density of state.[3] As a result, nonradiative relaxation and thermalization are restricted at certain electronic states because of the absence in phonon modes. Particularly, multi-phonon relaxation, which has much higher rate than that of the one phonon rate, is eliminated between the states separated by a small energy gap. For a nanocrystal of spherical shape, the low frequency normal modes are standing waves. The vibrational modes of a finite sphere were analyzed previously by Lamb[12] and Tamura et al.[13] To reveal the size dependence of phonon modes, we have calculated the PDOS for the low-energy phonon modes in nanocrystal of Y_2O_2S, which has a space group D_{3d}^3, and unit cell lattice constants of $a = 3.78$ Å, $c = 6.56$ Å. The reduced eigenvalues of acoustic phonon modes were calculated numerically and the $(2l + 1)$-fold degeneracy of the lth state and two vibrational modes were taken into account in the evaluation of the PDOS. The calculated PDOS in the Y_2O_2S crystals with a diameter of 20 nm is plotted in Figure 3(a). It is clearly shown that the phonon modes with energy less than 200 cm^{-1} are reduced significantly, and there are no phonon modes below 24 cm^{-1}. The cutoff energy reduces to 13 cm^{-1} for 40-nm crystals.

Because of the absence of low-energy phonon modes, nonraidative phonon relaxation of ions in certain electronic states is expected to be different from that in bulk materials.

The calculated PDOS suggests that, in the 20-nm crystals, direct one-phonon relaxation is restricted to the energies of discrete phonon modes, whereas for energy gaps less than 30 cm^{-1}, multiphonon relaxation is completely eliminated. The two-phonon Raman process becomes the dominant relaxation mechanism.[3,14,15] The equilibrium population in the upper levels of the $^4I_{15/2}$ ground state results from the competition mainly between the laser-induced thermalization (LIT) through nonradiative relaxation in the excited states (populating) and two-phonon Raman process (depopulating). The ratio of Er^{3+} population between the two ground levels is estimated as

$$\frac{N_1}{N_2} \approx \frac{W_{\mathrm{LIT}} + W_{\mathrm{Raman,abs}} + W_{21,\mathrm{abs}}}{W_{\mathrm{Raman}} + W_{21}} = e^{-\Delta E_{21}/kT} + \frac{W_{\mathrm{LIT}}}{W_{\mathrm{Raman}} + W_{21}} \quad (1)$$

where N_1, N_2 are the population density of the ground levels 1,2 respectively; W_{21} is the rate of the direct one phonon spontaneous emission between 2 and 1; W_{Raman}, and $W_{\mathrm{Raman,abs}}$ are the rates of two-phonon Raman emission and absorption, respectively. The emission rates of direct phonon process and two-phonon Raman process between the stark levels (1,2) can be calculated by simply replacing the ideal Debye continuous model of PDOS with the actual phonon density of states we calculated for the 20-nm sample.[14,15] In eq 1, W_{LIT} is the equivalent populating rate of laser induced thermalization that depends on the pump laser intensity and the multiphonon relaxation rates of W_{NR1} and W_{NR2} from the excited states $^4F_{7/2}$ and $^2H_{11/2}$ that allow multi-phonon relaxation between two energy gaps of 1206 and 741 cm^{-1}, respectively. In solids, the dominant nonradiative relaxation occurs with phonon energies near the Debye energy which is approximately 340 cm^{-1} for the Y_2O_2S lattice. On the basis of our calculation the PDOS in the high-energy side near Debye energy is nearly continuous. We assume that the phonons emitted during the Er^{3+} relaxation are absorbed locally and induce thermalization of Er^{3+} ions into the upper levels of the ground state with energies from 23 to 249 cm^{-1}. Therefore, we can estimate the value of W_{LIT} in the nanocrystals from

$$W_{\mathrm{LIT}} = k_0\frac{\sigma I_{\mathrm{p}}}{h\nu_{\mathrm{p}}}(W_{\mathrm{NR1}} + W_{\mathrm{NR2}}) \quad (2)$$

where $W_{\mathrm{NR1}} = W_{10}[1 - \exp(-302/kT)]^{-4}$ is for a four-phonon relaxation process, and $W_{\mathrm{NR2}} = W_{20}[1 - \exp(-247/kT)]^{-3}$ for a three-phonon relaxation process; k_0 is the scaling factor; I_{p} is the incident pump intensity; σ is the average absorption cross section of the pump laser.

At temperature below 10 K and for energy gaps larger than 20 cm^{-1}, the first term in eq 1 is negligible, and as shown in Figure 4(a) the upper level population is mainly due to the second term, whereas at temperature higher than 10 K, the sharp increase in the two-phonon Raman process suppresses the second term, thus the upper level population is due to the first term that obeys the normal Boltzmann distribution. For qualitatively elucidating the hot band dynamics, Figure 4(b) shows the estimated temperature dependence of the Er^{3+} population in the first excited crystal field level at 23 cm^{-1} above the ground level. In comparison with Figure 2, our calculation agrees very well qualitatively with the experimental results. Once the nonradiative relaxation significantly diminishes at low temperatures, Er^{3+} population will accumulate in the low-lying crystal field levels because at the same temperature the relaxation and

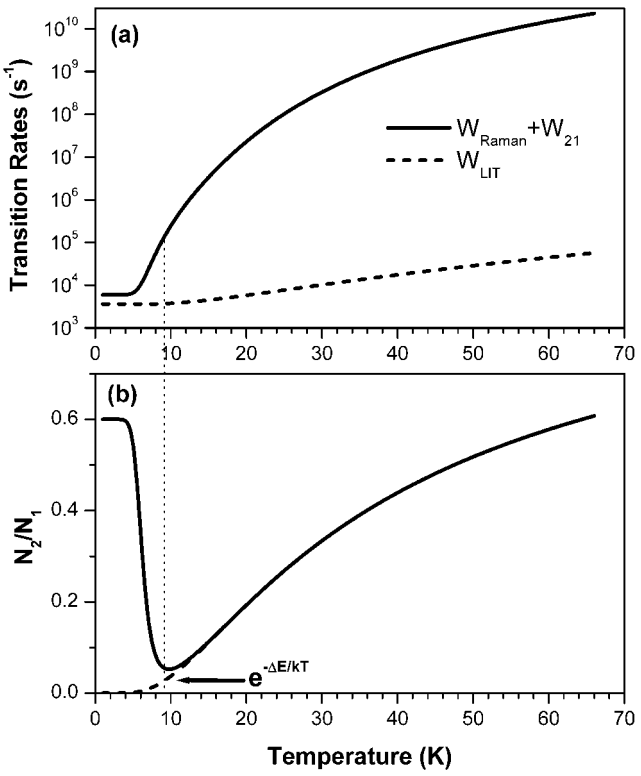

Figure 4. Calculated temperature dependence of (a) nonradiative relaxation and laser excitation induced thermalization, and (b) hot band intensity in nanocrystals of Er^{3+}:Y_2O_2S, for the crystal field level 23 cm^{-1} above the ground level.

thermalization of high-energy phonons generated by laser excitation from the ground state are not affected by the confinement effect. As a result, the intensity of the hot bands increases and saturation may occur when the Er^{3+} population in the ground state is depleted. At higher temperatures, both direct phonon relaxation and two-phonon Raman process become active, and the nanocrystals exhibit normal thermodynamics. The calculated anomalous temperature dependence applies to all hot bands shown in Figure 1, although quantitative reproduction of these hot bands as a function of temperature is not realistic because of many unknown parameters such as cross section and branching ratio for the radiative and nonradiative transitions involved in the hot band spectrum.

The anomalous thermalization effect due to absence of low-frequency phonon modes in nanocrystals should also occur generally in other systems. Observation of this effect depends on the energy level structure of the luminescence centers as well as the sample temperature and crystal size. According to the temperature-dependent multiphonon relaxation rate and the relationship between the cutoff frequency and crystal size, anomalous hot bands from the excited states with higher energies would occur in crystals with smaller size. We believe that the anomalous thermalization that Tissue [1] observed in nanocrystals of Eu_2O_3 is the same effect as we observed in Er^{3+}:Y_2O_2S. In the Eu_2O_3 nanocrystal, intensive hot bands observed in the excitation spectra of Eu^{3+} at 12 K were due to excitation of Eu^{3+} from three crystal field levels of the $^7F_1$ excited state (the ground state of Eu^{3+} is a singlet $^7F_0$). Because these excited states are at 300 cm^{-1} and higher above the ground state, diminishing multi-phonon relaxation requires that the crystals have much smaller crystal size so that phonon modes up to 150 cm^{-1} are eliminated. In Tissue's observation, the hot bands from the $^7F_1$ state are very strong in the crystals of 4 to 6 nm diameter, but become almost not observable in the crystals of 12 nm diameter. These results are consistent with our interpretation for the Er^{3+} system. Our hypothesis also predicts that the $^7F_1$ hot bands in the 4−6-nm Eu_2O_3 crystals would diminish as temperature increases up to 80 K when one-phonon direct relaxation and two-phonon Raman processes act more strongly in this system.[15]

Although modification of low energy phonon modes directly influences the fluorescence dynamics of rare earth ions in nanocrystal, the confinement on nonradiative relaxation in nanocrystals also influences the fluorescence dynamics through phonon-assisted energy transfer processes.[16−18] In general, energy migration and cross relaxation require low-energy phonons to match the energy difference between a donor and an acceptor. The absence of low-energy phonon modes in nanocrystals would reduce the energy transfer efficiency. It was shown that the Er^{3+} up-conversion efficiency in the Er^{3+} and Yb^{3+} codoped Y_2O_2S crystals of 20−50 nm diameters was only one-third of that in the 400 nm crystals.[5]

In summary, we have interpreted an anomalous thermalization effect that was observed in laser excitation of Er^{3+} in nanocrystals of Y_2O_2S. The dynamics of unusual hot bands in the Er^{3+} spectrum are analyzed based on the restricted phonon relaxation at low temperatures. Our analysis indicates that, for rare earth ions in dielectric nanocrystals, anomalous hot bands in low-temperature optical spectra should appear due to the lack of low-energy phonon modes. Given that Er^{3+} is an important optical activator of lasing medium, optical amplifiers, and up-conversion phosphors, and particularly for future nanophotonic devices, fundamental understanding of phonon confinement effects on its luminescence dynamics is of great importance.

Acknowledgment. The samples studied in this work were provided by S. Li of OraSure Technologies, Inc. This work was performed under the auspices of the Office of Basic Energy Science, Division of Chemical Sciences, the U. S. Department of Energy, under Contract No. W-31-109-ENG-38.

References

(1) Tissue, B. M. *Chem. Mater*. **1998**, *10*, 2837.
(2) Meltzer, R. S.; Feofiov, S. P.; Tissue, B.; Yuan, H. B. *Phys. Rev. B* **1999**, *60*, R14 012.
(3) Meltzer, R. S.; Hong, K. S. *Phys. Rev. B* **2000**, *61*, 3396.
(4) H.-S. Yang, Feofilov, S. P.; Williams, D. K.; Milora, J. C.; Tissue, B. M.; Meltzer, R. S.; Dennis, W. M. *Physica B* **1999**, *263−264*, 476.
(5) Li, S.; Feindt, H.; Sutorik, A. C.; Baliat, M. S.; Laine, R. M.; Niedbala, R. S. In. *Nanoscience and Nanotechnology in Perspective*, Liu, G. K., Wang, Z. L., Eds.; Tsinghua University Press: Beijing, in press.
(6) Bickmore, C. R. Waldner, K. F.; Baranwal, R.; Hinklin, T.; Laine, R. M. *J. Europ. Ceram. Soc.* **1998**, *18*, 287.
(7) Niedbala, R. S.; Vail, T. L.; Feindt, H.; Li, S.; Burton, J. L. *Proc. SPIE* **2000**, *3913*, 1605.

(8) Joubert, M. F.; Guy, S.; Jacquier, B. *Phys. Rev. B* **1993**, *48*, 10 031.
(9) Liu, G. K.; Chen, Y. H.; Beitz, J. V. *J. Lumin.* **1999**, *81*, 7.
(10) Rossat-Mignod, J.; Souillat, J. C.; Linares, C. *J. Phys. Chem. Solids* **1973**, *34*, 371.
(11) Carnall, W. T.; Fields, P. R.; Sarup, R. *J. Chem. Phys*. **1972**, *57*, 43.
(12) Lamb, H. *Proc. Math. Soc. London* **1882**, *13*, 187.
(13) Tamura, A.; Higeta, K.; Ichinokawa, T. *J. Phys. C* **1982**, *15*, 4975.; Tamura, A. *Phys. Rev. B* **1995**, *52*, 2668.
(14) Di Bartolo, B. *Optical Interaction in Solids*; John Wiley & Sons: New York, Ch. 15, 1968.
(15) Powell, R. C. *Physics of Solid-State Laser Materials*; Springer-Verlag: New York, 1998, ch. 4.
(16) Yen, W. M. In *Spectroscopy of Solids Containing Rare Earth Ions*; Kaplyanskii, A. A., Macfalarne, R. M., Eds.; North-Holland, Amsterdam, 1987, ch. 4.
(17) Huber, D. L.; Hamilton, D. S.; Barnett, B. *Phys. Rev. B* **1977**, *16*, 4642, Huber, D. L.; *Phys. Rev. B* **1979**, *20*, 2307.
(18) Hegaty, J.; Huber, D. L.; Yen, W. Y. *Phys. Rev. B* **1982**, *25*, 5638.

NL0255303